Naji, A., Warr, P. A., Beach, M. A., & Morris, K. A. (2011). A fundamental limit on the performance of geometrically-tuned planar resonators. IEEE Transactions on Microwave Theory & Techniques, 59(6), 1491 - 1499. 10.1109/TMTT.2011.2118227

A Fundamental Limit on the Performance of Geometrically-Tuned Planar Resonators

Adham Naji, *Member, IEEE,* Paul Warr, Mark Beach, *Member, IEEE* and Kevin Morris

***Abstract*—Geometric frequency tuning in planar electromagnetic resonators is common in many applications. It comes, however, at a penalty in the resonance quality, Q_0. The literature traces the causes of such penalty often in terms of the shortcomings in the added elements and materials, which were used to achieve the tuning. In this paper, however, it is shown that another underlying source of quality degradation exists at the fundamental geometric level. This source, unlike other added sources of degradation during tuning, will always exist (even before tuning takes place) and will rely on the 'modal areas' of the geometric modifications made to host the tuning mechanism. It hence forms an upper bound to the performance that can be achieved from a geometrically-tuned planar resonator, carries an important insight to resonator design in general and significantly helps understanding the problem of geometric tuning in particular. We present the electromagnetic theory behind this limit and canonically demonstrate it using practical microwave resonator examples. The theory, Finite-Element Method simulation and experiment results are presented and good agreement is observed. It is shown that incorporating such understanding into the design process of tunable planar resonators can help optimize their performance against a given set of design requirements. Furthermore, the presented theory provides a useful electromagnetic model as a tool for estimating the Q_0 for geometrically-modified or irregular metal patches and planar resonators in general, to assist analysis and design at any wavelength or application. The theory also asserts that, under a given mode, a planar resonator will always have its maximum Q_0 before introducing any internal subtractive geometric modifications (e.g., cuts, apertures or slits) to its original shape.**

***Index Terms*—Tunable Resonators, Tunable Filters, Unloaded-Q, Planar Resonator, Frequency Tuning, Microstrip Resonator, Design Optimization, Millimeter Resonators, Applied Electromagentism.**

I. Introduction

TUNING electromagnetic resonators to change their resonant frequencies is desirable and common in many fields and applications. As resonators usually form the building blocks of many physical systems, such as various filter structures, antennas, optical and imaging devices (to mention a few), their performance is often critical to the overall system operation [1]–[6]. A classic problem that normally accompanies resonator tuning attempts, however, is the degradation of resonance quality as the tuning takes place. Often such degradation worsens as the tuning range widens with respect to the initial point of resonance, at which the structure was designed to be optimal [7].

A common method of tuning (discussed below) is to change the geometric shape of the resonating structure in a given material, as to resonate at a different frequency (or wavelength). Yet, all known attempts that use tuning elements to help the structure adapt in shape are known to have degrading effects on the quality of resonance. As a result, focus is usually given to optimizing these added tuning elements. In this paper we pay attention to another, more-inherent source of degradation, which is the geometrical modification itself and its specific design, which is found to dictate key performance limits, enhance the understanding of the tuning problem and carry significant insight to the design aspects of tuned planar resonators in general. We discuss the theory behind this important source and demonstrate it with practical examples.

To demonstrate this general principle in a feasible manner, we apply the theory developed herein onto planar resonators in the microwave region. In this region the device sizes that correspond to the resonating wavelengths, using conventional materials, have often been found useful for radiating power or storing electromagnetic energy without significant loss, in addition to being physically convenient to handle and easy to fabricate [8]–[10]. In fact, it is interesting here to note that many fields in physics and engineering that deal with wave phenomena at various scales, such as optics, acoustics, radio engineering, super-resolution microscopy, imaging, metamaterials and transformation optics, have benefited from the mutual resemblance with microwave systems to demonstrate or share common principles (e.g., [1], [4], [9]–[14]). This fact also stems from the canonical generality (and complexity) of wave theory (from Maxwell's equations) at the microwave frequencies [13].

II. Geometric Tuning

Since, in a given material, a resonant structure is defined by its physical dimensions, its function is generally attributed to its geometry. Due to this fact, electromagnetic or microwave systems and circuits are often described as distributed (as opposed to lumped) in nature [1], [4]. When it is desirable to make such a system tunable in frequency ($f = \upsilon/\lambda$), it is then implied that a mechanism must be found to modify its geometry (to change the value of λ) or its material properties (to change the value of υ), relative to one another. Where υ is the velocity of propagation and λ is the resonant wavelength. This change will result in a structure that resonates at different frequencies. Such attempts for achieving tuning

A. Naji is with the Department of Electrical and Electronic Engineering, University of Bath, England; e-mail: a.naji@bath.ac.uk. P. Warr, M. Beach and K. Morris are with the Department of Electrical and Electronic Engineering, Center for Communication Research (CCR), University of Bristol, England. e-mail: paul.a.warr@bristol.ac.uk.

This research was jointly funded by EPSRC and MobileVCE.

Manuscript received August, 2010.

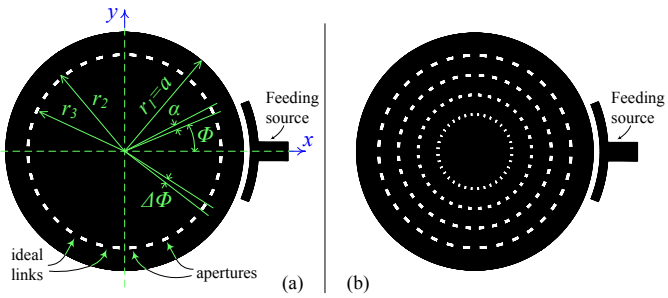

Fig. 1: (a) A canonical example of geometric tuning in a circular disk and (b) its extension into multiple (four) layers.

can be seen in abundance in the literature. Although changing the material properties (e.g., ferroelectrics) is used feasibly under some scenarios, the second method that uses geometric tuning is far more applicable and more flexible. This fact is also reflected in the literature on microwave resonators [6], [7], [9], [13], [15]. (Common examples include the use of PIN diode switches or Micro-ElectroMechanical System (MEMS) switches, which switch between different geometric configurations, providing different overall apparent shapes of the resonator.) The term 'geometric tuning', in this paper, refers to any shape modifications applied to the distributed face of the planar resonator (along its plane) to change its apparent shape from its original condition. We do not consider, hence, tuning mechanisms that utilize lumped tuning techniques, such as varactors (which tune lumped capacitance, not shape) or switches that shunt across the substrate (rather than along the resonator's surface plane). Since the discussion herein is about pre-defined resonator shapes, its also implied that the introduced geometric modifications are in fact subtractive (not additive) to the original shape and occur within its original boundaries (i.e., internal). For example, apertures or slits inside a patch resonator are considered, but not the addition of a metallic extension outside the patch's original contour.

When microwave resonators are geometrically tuned in such a manner, one tangible and consistent problem is always observed: the degradation in resonance quality, which accompanies the tuning. Although the exact amount of quality degradation (compared to its value before tuning) is dependent on the particular scenario of implementation, its sources have generally been traced back in the literature to a few key limitations [7], [16]–[18]: imperfections in the utilized materials or techniques, introduced losses and distortion due to switching elements and, most importantly, increased impedance mismatch with other parts of the system due to the introduction of tuning. The last cause, in particular, stems from the fact that matching is an inherently frequency-dependent process. Hence, usually a change in resonant frequency will imply losing the previously-optimized electromagnetic coupling that once existed between the resonator and its feeding source (or connected load) before tuning. This would cause a system's impedance to mismatch, unless some complex techniques are added to compensate for this effect.

III. Inherent Q_0 Limit

Given an initially fixed structure that resonates at a given frequency f_0, its resonance quality at f_0 will degrade merely due to any geometric modifications that are applied internally to that structure, *even* if the techniques used for achieving the geometric tuning are of ideal characteristics and the impedance matching to the system is maintained. Having non-ideal tuning techniques or imperfect material characteristics will only add further degradation to this upper bound (limit) on performance. Furthermore, this degradation in quality will occur due to the mere installation of the subtractive geometric tuning mechanism to the resonator's face, *even* if tuning has not yet taken place (i.e., at the same frequency). This point indicates that the initial structure prior to these modifications will always have the maximum Q_0, and any internal modification will decrease Q_0, even if tuning is not sought. Using a simple method of calculation, it is shown that Q_0 will degrade depending on the relative locations and sizes of the geometric modifications within the surface of the structure and as seen by the resonating mode. The total effect is called the 'modal-area' of these modifications, which is the sum of such areas from the perspective of the resonant mode (Section IV). This result carries important implications to different aspects regarding the design of tunable resonators, or any other electromagnetic structure that is related to (or inspired from) such resonant structures, in the different fields of physical sciences and engineering. Examples include structures that carry geometric patterns, random defects, or even periodic and fractal geometric effects.

IV. Theory

We consider one of the most common (and convenient) types of modern resonating structures, the planar structure, where geometric modifications can be applied internally to a metallic surface of a resonator. The metallic surface is typically lithographically-etched or machined (depending on size and accuracy) on a dielectric substrate, which lies above a ground plane. The resonance quality is succinctly expressed using the unloaded-quality factor Q_0 at resonance. This metric is very powerful for characterizing the performance of the resonator itself, rather than the system parts coupled to it. Effectively, by using Q_0, the effects of any impedance matching or coupling coefficients are not taken into consideration [1], [4], [19], [20].

As an example, consider the canonical case of a metallic disk patch of radius a, on a substrate with a complex relative permittivity $\epsilon_r' - j\epsilon_r''$ and height h, positioned above a ground plane (a microstrip structure). Geometric tuning can be applied for tuning the resonant frequency of this resonator by making a narrow ($r_2 - r_3 = \Delta r << \lambda$) annular aperture (slit) in the metallic patch, and then bridging this aperture with links (switches), which are removable, as in Fig. 1(a). The operation is simple, when the links are present, the structure appears to be one solid disk with radius a; when the links are removed, it appears as a ring with radii a and r_2 and a separate smaller disk with radius r_3. The two cases offer two different frequencies, one for the whole disk and one for the ring. Note that this can be further iterated into multiple layers of rings, to give more

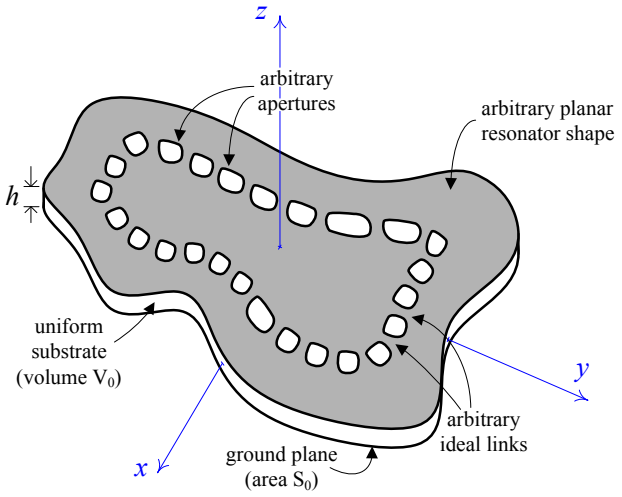

Fig. 2: A general arbitrary planar resonator with arbitrary geometric modifications applied to it.

tuning steps and more complex structures, as in Fig. 1(b) for example. We wish to ascertain whether Q_0 degrades due to these modifications, even if those links were chosen to be ideal elements, and before any tuning. That is, even when the links are present and the structure resembles its original solid form, with radius a and at the same resonant frequency f_0, we would like to know if Q_0 will degrade and, if so, according to what law. In effect, the links are chosen to be metallic contacts made from the same metal as the original patch, with the aperture etched away photolithographically. This will provide the ideal links for the comparison of the performance before and after the addition of this tuning mechanism (all at f_0). Note that the use of the unloaded-Q, on the other hand, automatically drops from consideration any contribution in quality degradation from the system coupling or impedance mismatching.

Before analyzing this canonical example, however, we first consider the general arbitrary case of Fig. 2.

The unloaded-Q is known in general as

$$Q = \frac{\omega \cdot \text{average EM-stored energy}}{\text{lost power}} = \frac{\omega(W_e + W_m)}{P_l}, \quad (1)$$

where ω is angular frequency ($= 2\pi f$), W_e and W_m are the average stored electric and magnetic energies, respectively, and P_l is the total lost power in the structure. At resonance, $\omega = \omega_0$, it is known that W_e becomes equal to W_m. Also, P_l will comprise different mechanisms of loss; mainly, power loss in the imperfect dielectric (due to ϵ_r''), P_{l_d}, power loss due to conductor surface resistance (R_m), P_{l_c}, and power lost to radiation, enclosure, or other losses and stray couplings from the edge of the resonator, P_{l_r}. Hence, Q at resonance becomes

$$Q_0 = \frac{2\omega_0 W_e}{P_{l_d} + P_{l_c} + P_{l_r}}. \quad (2)$$

Usually the axial thickness of the substrate (along axis z) is relatively much smaller than its cross-sectional area (planar area in the xy-plane) and λ, and no field variations are considered along the z-axis. Therefore, modes that usually dominate such planar structures are Transverse Magnetic (TM) modes, denoted TM^z_{mnp}, with $p = 0$, while m represents the variations along x and n the variations along y. Prior to the application of geometric tuning to this general structure, the energy stored in the resonator's volume, V_0, the power lost in its dielectric, and the power lost along both its conductive surfaces, each with area S_0, are

$$W_e = \frac{\epsilon_0\epsilon_r'}{4}\int_{V_0} \boldsymbol{E}\cdot\boldsymbol{E}^*\, dV = \frac{\epsilon_0\epsilon_r' h}{4}\int_{S_0} |E|^2\, dS \quad (3)$$

$$P_{l_d} = \frac{2\omega_0\epsilon_r''}{\epsilon_r'} W_e \quad (4)$$

$$P_{l_c} = 2\frac{R_m}{2}\int_{S_0} \boldsymbol{J}\cdot\boldsymbol{J}^*\, dS = R_m \int_{S_0} |H|^2\, dS = R_m \frac{\epsilon_0\epsilon_r'}{\mu_0\mu_r}\int_{S_0} |E|^2\, dS \quad (5)$$

since, $\int_V dV \equiv \int_0^h dz \int_S dS = h\int_S dS$, and at resonance we have

$$\frac{\mu_0\mu_r'}{4}\int_V \boldsymbol{H}\cdot\boldsymbol{H}^* dV = W_m = W_e = \frac{\epsilon_0\epsilon_r'}{4}\int_V \boldsymbol{E}\cdot\boldsymbol{E}^* dV$$

$$\Rightarrow |H|^2 = \frac{\epsilon_0\epsilon_r'}{\mu_0\mu_r}|E|^2. \quad (6)$$

Where E, H and J are the electric field, magnetic field, and current density, respectively, with boldface symbols representing vectors.

It is important to note that the quality factor is defined per resonant frequency (i.e., at one distinct mode, or a number of degenerate modes, where applicable). Therefore, one can base all the calculations on the original resonant angular frequency, ω_0, of the original structure. Once the geometric modifications are applied (i.e., the arbitrary apertures in Fig. 2 are made), the operating mode in the resonator encounters additional discontinuities in its path. These can be clearly observed (or envisaged) by considering the paths of the surface currents at the top metallic patch. Perturbation theory [2], [4], [13] implies that, as a first approximation, the disturbance negligibly affects the nature of the propagating mode, as the modifications remain much smaller than the operating wavelength, λ. Thus, the original dominant mode remains dominant (see for example the mode distributions in Fig. 3). The discontinuities, however, have an effect on the spacial prevalence of that mode, compared to its original state. Specifically, the modal surface currents will no longer pass through the gaps (apertures) in the metallic patch, and the electromagnetic field guided within the substrate underneath it will behave in harmony with this and with the new setup of boundary conditions. In effect, apart from some fringing field's margin near the edges of the apertures, the field now is discouraged from occupying or delivering any net electromagnetic power into the volumes directly beneath the apertures under the current mode; as can be readily found using the Poynting's theorem for average power flow into such volumes. These topical effects, which can be seen collectively as directing the surface currents into passing through the links bridging the apertures, are merely

the net effect of the overall account that involves higher and/or evanescent mode excitations in the vicinity of the introduced discontinuities. The original mode loses some of its energy (ΔW_e) feeding such mode conversion, regardless of whether such modes would be supported further by the overall structure. The amplitude of the original mode's field will thus be reduced by some conversion factor $\xi \in [0,1]$, due to encountering the discontinuities. The loss of amplitude will feed other modes, whose emerging amplitudes can be found using Lorentz's Reciprocity Theorem [2]–[5]. This gives new power loss terms (dielectric, conductors, and radiation losses) from such modes as

$$P_{lnew} = \sum_t P_{l_{d,new}} + \sum_t P_{l_{c,new}} + \sum_t P_{l_{r,new}} = P_l \cdot \xi^2, \quad (7)$$

where t is an arbitrary index that covers all the new modes considered from mode conversion. The dominant mode will have a new Q_0 value, donated $\breve{Q}_0$, as follows

$$\breve{Q}_0 = 2\omega_0 \frac{\breve{W}_e}{\breve{P}_l} = 2\omega_0 \frac{W_e - \Delta W_e}{P_l - \Delta P_l + P_{l_{new}}}, \quad (8)$$

$$\text{where} \quad \Delta P_l = P_l \cdot \xi^2,$$
$$\Delta W_e = \frac{\epsilon_0 \epsilon_r'}{4} \sum_{j=1}^{N} \int_{\Delta V_j} |E|^2 dV,$$

N denotes the total number of apertures or links, ΔV_j denotes the volumes that lie directly beneath the arbitrary apertures (each indexed with an index j), and ΔP_l is the reduction in the original lost power due to the reduction in the field amplitude (ξ).

Since the reference in equation (8) is to the original mode, any power that passes via mode conversion to other modes is considered lost power from this mode. Therefore, although the losses P_l have reduced by some amount (ξ^2) due to the reduction in amplitude of the field, there is also an increase in wasted power elsewhere by the same amount (ξ^2). Thus, in total, $\Delta P_l \approx P_{l_{new}}$ and $\breve{P}_l \approx P_l$. The reduced amplitude of the field has thus affected mainly the stored energy under that mode (by ΔW_e), rather than the losses P_l. Then

$$\breve{Q}_0 = 2\omega_0 \frac{W_e - \Delta W_e}{P_l} = 2\omega_0 \frac{\delta \cdot W_e}{P_l}, \quad (9)$$
$$\text{where: }]0,1] \ni \delta = \frac{W_e - \Delta W_e}{W_e},$$

because having δ equal to zero would mean that the resonant structure has vanished (an inadmissible value).

This definition leads to

$$\Rightarrow \delta = \frac{\int_{V_0} |E|^2 dV - \sum_{j=1}^{N} \left(\int_{\Delta V_j} |E|^2 dV \right)}{\int_{V_0} |E|^2 dV}$$
$$= 1 - \frac{\sum_{j=1}^{N} \left(\int_{\Delta S_j} |E|^2 dS \right)}{\int_{S_0} |E|^2 dS} = 1 - \gamma, \quad (10)$$

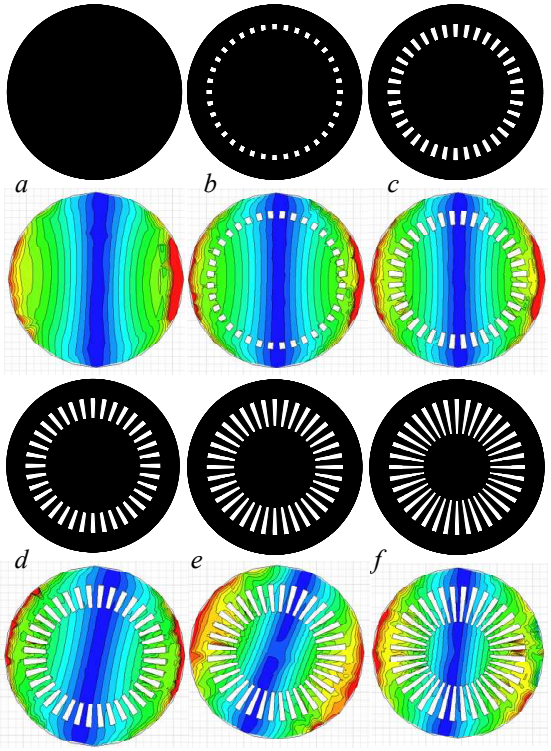

Fig. 3: Examples of different Δr gaps applied to the circular resonator: (a) Δr=0 mm, (b) Δr=1 mm, (c) Δr=2 mm, (d) Δr=3 mm, (e) Δr=4 mm, (f) Δr=5 mm; all on a Duroid substrate with $\epsilon_r' \approx 6.15$, $\epsilon_r'' \approx 0.0068$, $h = 1.27$ mm, $\alpha = 5°$, $N = 36$ links, $r_1 = a = 12$ mm, $r_2 = 9.5$ mm, 0.5 oz. of Copper cladding for both ground plane and resonator face, and each structure is enclosed inside an Aluminum enclosure with dimensions 50 mm $\times$ 50 mm $\times$ 31 mm. The lower part of each tuning step shows the normalized E-field modal distribution (color scale between red (highest value) and blue (lowest value)). Note how the general features of the dominant mode are still maintained across the structure.

where γ is called the normalized modal-area of the modifications.

This important result does not only provide a simple theoretical method for approximately evaluating $\breve{Q}_0$ after the introduction of geometric modifications (for tuning or other purposes), but also shows that $\breve{Q}_0$ will always be less than Q_0, as $\breve{Q}_0/Q_0 = \delta$. Furthermore, it shows that the rate of degradation in Q_0 as the modifications on the resonator's surface increase ($\partial\delta/\partial S$) will depend on the spatial variations (i.e., as a function $f(x,y)$) of the mode and on the size and position of these modifications with respect to that mode. The curve of Q_0 as a function of these modifications will thus be always rolling down, with its rate of decrease depending on the specific implementation in hand. This can also provide insight into how to build geometrically-tuned resonators in an optimal manner, for any specific wavelength, spectrum, or application. Indeed, some applications might intentionally require wider bandwidths (lower Q_0) from the same resonator and opt to choose their geometric tuning mechanism as to give Q_0 curves

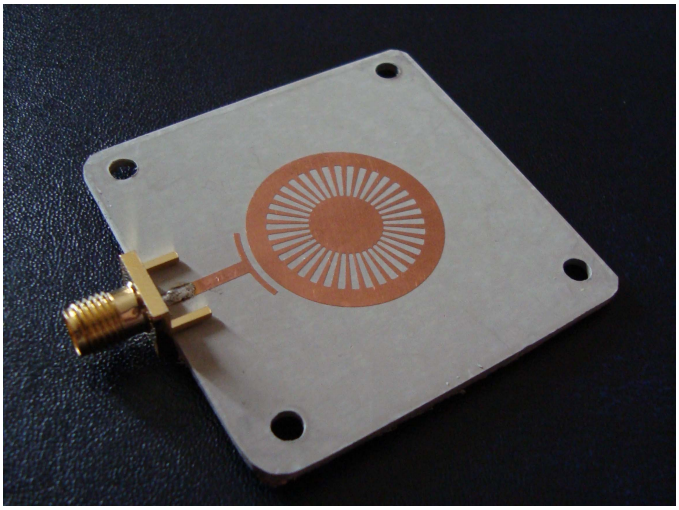

Fig. 4: An indicative photograph of case (f) in Fig. 3 with Δr=5 mm; the Aluminum enclosure (dimensions 50 mm $\times$ 50 mm $\times$ 31 mm) is removed in this photograph.

that roll down quicker with the size, shape or position of the made modifications (and vice versa). Furthermore, this result provides a useful electromagnetic model as a tool for estimating Q_0 for geometrically-modified or irregular metal patches and resonators in general, to assist analysis and design for any wavelength or application.

The characteristic reduction in Q_0 due to geometric modifications can be physically explained by the structure's decreased ability to store electromagnetic energy, although its effective surface currents and losses are approximately fixed. Since these currents/losses at microwave frequencies are often attributed to the structure's surfaces, whereas the energy storage is attributed to the structure's volume [21], the net effect of geometric tuning can then be approximately viewed as an action that affects the structure's apparent volume at a much larger rate than affecting its surface area. This causes the ratio between the effective volume and effective surface area of the resonator to decrease and a degradation in Q_0 is observed.

Note that the relatively small volumes of the links (switches) in practice will be negligible in terms of storing any electromagnetic energy (if any was being offered in their vicinity). This is particularly the case in the geometric modifications considered here, where these tuning elements are at the surface plane of the resonator (not shunt) and since their forward stray capacitance and inductance values are usually negligibly small.

V. A Canonical Example

To indicate how this method can be implemented, we now apply these findings onto the canonical example of Fig. 1(a). The circular structure was chosen for its attractive features [22]–[24] of having less fringing losses and discontinuities, due to its smooth shape (compared to rectangular shapes, for example). In this case, we consider the field of the dominant mode $\mathrm{TM}^z_{n_\phi m_r 0}$ = TM^z_{110}, which is given in a cylindrical frame of coordinates as

$$E_z = CJ_1[kr]cos(\phi), \tag{11}$$

$$H_\phi = \frac{-jCk}{k_0 Z_0} J_1'[kr]cos(\phi), \tag{12}$$

$$H_r = \frac{-jC}{k_0 Z_0 r} J_1[kr]sin(\phi), \tag{13}$$

where, $j=\sqrt{-1}$, C is an arbitrary amplitude constant, $J_q[.]$ is Bessel's function of the first kind and of degree q, $J_q'[.]$ is the derivative of $J_q[.]$ with respect to its argument, k is the wavenumber, $k_0 = k/\sqrt{\epsilon_r'}$, Z_0 is the wave impedance (120π), and (r, ϕ, z) are the cylindrical coordinates frame's variables.

In this case we find, after some mathematical manipulation [4], that the pre-tuning values are

$$W_e = |C|^2 \frac{\epsilon_0 \epsilon_r'}{4} \int_0^h \int_0^{2\pi} \int_0^a J_1^2[kr]cos^2(\phi) r dr d\phi dz$$

$$= |C|^2 \frac{\pi \epsilon_0 \epsilon_r' h}{4} \frac{a^2}{2} \left\{ \left(1 - \frac{1}{k^2 a^2}\right) J_1^2[ka] \right\} \tag{14}$$

$$P_{l_d} = \frac{\omega_0 \epsilon_r'' \epsilon_0}{2} \int_V \boldsymbol{E} \cdot \boldsymbol{E}^* dV = \frac{2\omega \epsilon_r''}{\epsilon_r'} W_e \tag{15}$$

$$P_{l_c} = |C|^2 \frac{R_m}{k_0^2 Z_0^2} (\pi) \int_0^a \left\{ k^2 J_1'^2[kr] + \frac{1}{r_2} J_1^2[kr] \right\} r dr$$

$$= |C|^2 \frac{R_m \pi}{k_0^2 Z_0^2} k^2 \frac{a^2}{2} \left(1 - \frac{1}{k^2 a^2}\right) J_1^2[ka]. \tag{16}$$

while the value of P_{l_r} is dependent on the enclosure or surroundings of the resonator (implementation-dependent). Applying equation (10) to this case, summing over all apertures, and after some mathematical manipulation, we get the degradation due to tuning as

$$\gamma = \underbrace{\frac{N\Delta\phi}{2\pi}}_{\text{angular ratio}} \underbrace{\frac{\left[\frac{r^2}{2}\left\{J_1'^2[kr] + \left(1 - \frac{1}{k^2 r^2}\right) J_1^2[kr]\right\}\right]_{r_3}^{r_2}}{\frac{a^2}{2}\left(1 - \frac{1}{k^2 a^2}\right) J_1^2[ka]}}_{\text{radial ratio } (\textit{non-linear})}. \tag{17}$$

Where $\Delta\phi$ is the angular span of each aperture between two adjacent links.

In one particular implementation (see Figs. 3, 4 and 5), the calculated $\breve{Q}_0$ from the theory above was compared with both Finite-Element Method (FEM) computation (using the HFSS full-wave electromagnetic field solver [25]) and laboratory experiments. The results exhibit good agreement within the fabrication and FEM-numerical tolerances (circa $\pm 3\%$ and $\pm 1\%$ maximum error in f_0, respectively) and within the marginal errors expected due to the complex nature of the fringing fields in the vicinity of each aperture. Practical methods that use non-ideal components to achieve the tuning (e.g., RF switches) will always produce Q_0 values which are below this fundamental limit and within the 'admissible zone' shown in Fig. 5.

In the theoretical model above, f_0 was continuously recalculated (refined) for each value of aperture spacing in appreciation of Cavity Perturbation Theory [1], which accounts for slight shifts in f_0 to maintain the electric/magnetic stored energies stand-off whilst the structure is perturbed. Also, the complex internal fringing in the radial direction over the

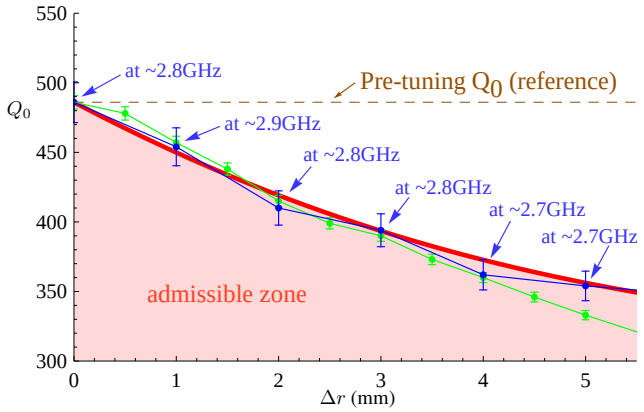

Fig. 5: A comparison between the theory predictions (red), the FEM simulation (green), and the experimental (blue) results for the circular resonator using: an aluminum enclosure with dimensions 50 mm × 50 mm × 31 mm, copper metallic resonator and ground plane (0.5 oz.), $\epsilon_r' \approx 6.15$, $\epsilon_r'' \approx 0.0068$, $h = 1.27$ mm, $\alpha = 5°$, $N = 36$ links, $r_1 = a = 12$ mm, $r_2 = 9.5$ mm, and r_3 as variable. The upper bound forms the maximum of the admissible zone, where the practical values of Q_0 will be in any practical geometric tuning (after further degradation is added due to the materials or the elements used to achieve the tuning). Fabrication and FEM-numerical tolerances resulted in maximum errors circa $\pm 3\%$ and $\pm 1\%$, respectively.

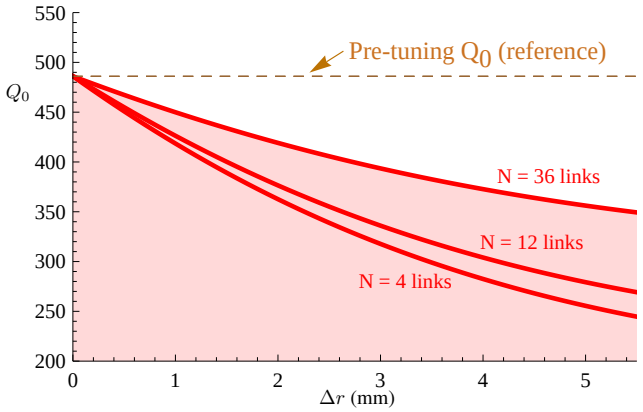

Fig. 6: A comparison between the theory predictions for three cases with different number in links (N = 4, 12, 36 links), of the circular resonator. For each case, the quality reduced as a function of increased gapping (Δr), but the cases with less number of links exhibited more degradation. This provides an insight into how to choose the number of links (N) correctly to meet a given set of requirements. The setup used an aluminum enclosure with dimensions 50 mm × 50 mm × 31 mm, copper metallic resonator and ground plane (0.5 oz.), $\epsilon_r' \approx 6.15$, $\epsilon_r'' \approx 0.0068$, $h = 1.27$ mm, $\alpha = 5°$, $N = 36, 12, 4$ links, $r_1 = a = 12$ mm, $r_2 = 9.5$ mm, and r_3 as variable.

apertures was approximately considered in terms of 'effective' gap sizing. Since the usual model that calculates such effects [22], [26] is actually linear with gap sizes but for simpler cases of lines, the method used in this model was to consider the effective-ratio for the largest value of gapping (Δr) and then map it linearly onto the rest of the gapping values to give a reasonable approximation of the fringing.

The measured data for Q_0 were deduced from the measurements of the single-port reflection scattering parameters, using the standard method in [20]. This method relies on measuring the loaded quality factor, Q, from the S_{11} curves and the coupling co-efficient from both the S_{11} curves and the Smith chart locii at resonance. The found coupling co-efficient is then de-embedded from the value of the loaded Q, to give the unloaded quality factor, Q_0. The Vector Network Analyzer 37397C from Anritsu was used to measure the S parameters, after calibrating it using the standard Open-Short-Terminated-Thru procedure.

Note that had the geometric tuning to this resonator been done with a different style, position or shape of geometric modifications, the rate of decrease of the Q_0 curve would have been different. For example, another test was carried out on this structure, but with a varying number of links (N = 4, 12, 36). The theory predicts that the reduction in the upper limit is as shown in Fig. 6. Figs. 7 and 8 show the agreement between the predicted and measured results for N = 12 links and N = 4 links, respectively. The theory can thus be useful in advising on the number of links required for a given set of design requirements (without using too many or too few links).

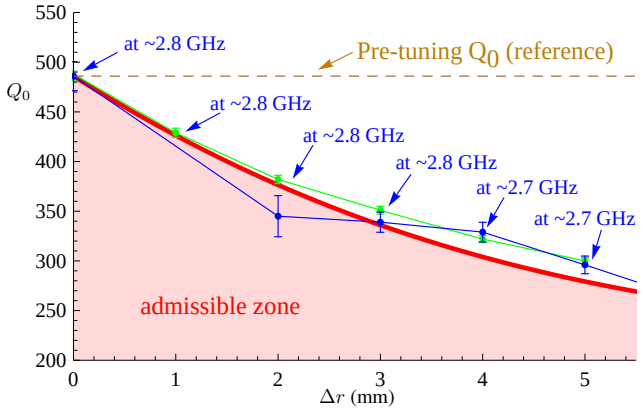

Fig. 7: A comparison between the theory predictions (red), the FEM simulation (green), and the experimental (blue) results for the circular resonator using: an aluminum enclosure with dimensions 50 mm × 50 mm × 31 mm, copper metallic resonator and ground plane (0.5 oz.), $\epsilon_r' \approx 6.15$, $\epsilon_r'' \approx 0.0068$, $h = 1.27$ mm, $\alpha = 5°$, $N = 12$ links, $r_1 = a = 12$ mm, $r_2 = 9.5$ mm, and r_3 as variable. The upper bound forms the maximum of the admissible zone, where the practical values of Q_0 will be in any practical geometric tuning (after further degradation is added due to the materials or the elements used to achieve the tuning). Fabrication and FEM-numerical tolerances resulted in maximum errors circa $\pm 3\%$ and $\pm 1\%$, respectively.

Fig. 8 also shows how, indeed, the imperfections of a commercial switching element (in this case, PIN diode BAP50-03 from NXP Inc. [27], which was biased to forward resistance of approximately 2 Ω and has a package size circa 2 mm ×

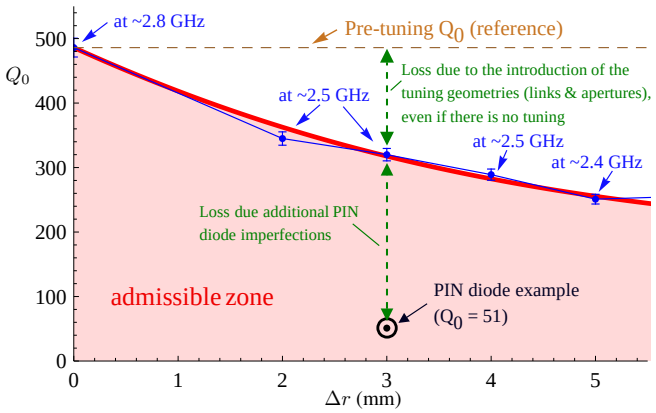

Fig. 8: A comparison between the theory predictions (red) and the experimental (blue) results for circular resonator using only 4 ideal links. Also shown is a measured value of Q_0 that falls within the admissible zone when the 4 links are replaced with commercial PIN diodes BAP50-03 from NXP Inc. [27], which were biased to forward resistance of approximately 2 Ω and has package size circa 2 mm × 1.2 mm × 1 mm. The setup also used an Aluminum enclosure with dimensions 50 mm × 50 mm × 31 mm, copper metallic resonator and ground plane (0.5 oz.), $\epsilon_r' \approx 6.15$, $\epsilon_r'' \approx 0.0068$, $h = 1.27$ mm, $\alpha = 5°$, $N = 4$ links, $r_1 = a = 12$ mm, $r_2 = 9.5$ mm, and r_3 as variable. Fabrication tolerances resulted in maximum errors circa ±3%.

1.2 mm × 1 mm) drive Q_0 to fall in the admissible zone, much below the upper limit, as expected. The biasing of these practical switches was designed to introduce a minimum of disturbance to the electromagentic field in the vicinity of the resonator. Thus, it was chosen that the bias wires be extended along the electric-wall mid-axis, which runs through the disk and is perpendicular to the line along the feedline (as the local maxima of the $|E|$ field occur near the feed edge). Fig. 9 shows the mode distribution and the electric-wall. According to Faraday's law (Maxwell's first equation) in its integral form

$$\int_S \nabla \times \boldsymbol{E} \cdot \boldsymbol{dS} = \oint_{\text{Contour}} \boldsymbol{E} \cdot \boldsymbol{dl} = \int_S -\frac{\partial \boldsymbol{B}}{\partial t} \cdot \boldsymbol{dS}, \qquad (18)$$

one can observe that the electromotive force would only be induced along these bias wires if the magnetic flux ($\boldsymbol{B}$) could cross past its circuit loop (normal to the wire), which is an absent condition when the wires are aligned along the electric-wall. Experiments that used this setup (see Fig. 10a) confirmed this by observing only a slight reduction in Q_0 (less than 2%) due to these wires. On the other hand, if the wires were aligned along the magentic-wall, much more coupling would occur and Q_0 would reduce significantly (by circa 20%).

To indicate how the inherent quality of a resonator can translate into performance parameters within other encompassing systems, such as antennas or filters, 4 dual-mode resonators were designed to give, at different Δr gap sizes, the same frequency, bandwidth and VSWR (matching). This was achieved by adjusting some design parameters in the layout shown in Fig. 11 among the 4 cases of Δr = 0, 1, 3, 5 mm.

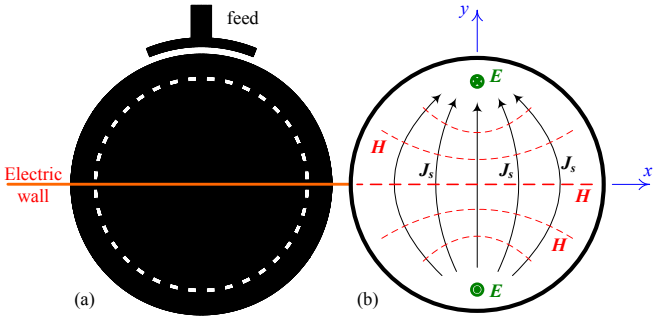

Fig. 9: The alignment of the bias-wires along the electric-wall of the structure, parallel to the magnetic flux, will result in the minimum induction of microwave current along the wires, according to Faraday's law (equation (18)). Note that the electric-wall is perpendicular to the feedline axis, which tends to pull the maxima of the $|E|$ field towards the feed position.

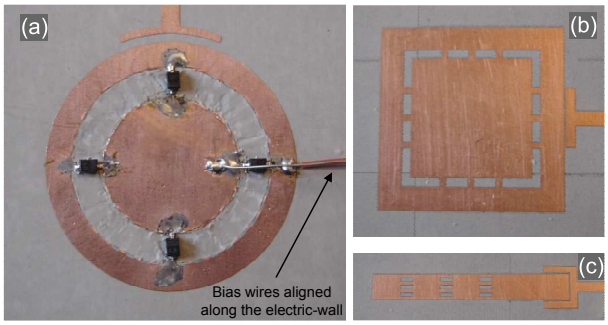

Fig. 10: Realizations of (a) the circular resonator with 4 links using the BAP50-03 PIN diodes from NXP and with bias-wires (each 0.25 mm in diameter) aligned along the electric-wall; (b) a square patch resonator example with ideal links; and (c) a line resonator example with ideal links.

Since the definition of Q is only valid and meaningful at a specific frequency, and since the coupling conditions (affecting matching and bandwidth) were also similar across the 4 cases, varying Δr among these resonators to reduce the Q_0 (as in Fig. 3) should result in worsening Insertion Loss (IL). Indeed, Fig. 12 shows FEM results that verify these expectations, and show that a reduction in Q_0 from 220 to 141, which is around -1.9 dB, corresponded to approximately 2 dB degradation in IL. The reduction in Q_0 at the resonator level has thus translated to degradation in IL at the filter system level. Note that coupling had to be critical as to bring the two degenerate modes of resonance under one frequency peak. Also note that the feeds were embedded within 'pocket' regions within the patch, near the edges, to increase the coupling to the required level and transfer sufficient energy to the resonator from the source (Fig. 12).

VI. Other Practical Examples

This section briefly shows how one can also apply the findings of this theory to other resonator shapes, which further

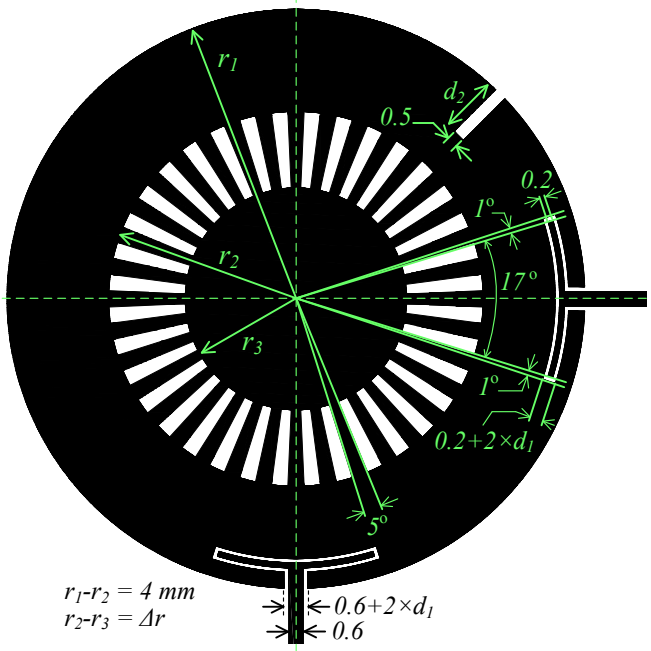

Fig. 11: The layout of the basic structure of the four dual-mode filters realized. This design was iterated 4 times, with each time having a different size of gapping: Δr = 0, 1, 3, 5 mm. The other parameters, namely, d_1, d_2 and r_1, were re-adjusted at each case, so that all the cases would produce the same frequency (required by the definition of Q_0), the same bandwidth and matching (S_{11} values) to allow for their Insertion Loss (IL) comparison. With Δr = 0 mm: d_1 = 0.15 mm, d_2 = 2.7 mm and r_1 = 12 mm. With Δr = 1 mm: d_1 = 0.18 mm, d_2 = 2.65 mm and r_1 = 11.96 mm. With Δr = 3 mm: d_1 = 0.165 mm, d_2 = 2.3 mm and r_1 = 11.35 mm. With Δr = 5 mm: d_1 = 0.162 mm, d_2 = 1.9 mm and r_1 = 10.43 mm. The setup also used an Aluminum enclosure with dimensions 50 mm × 50 mm × 31 mm, copper metallic resonator and ground plane (0.5 oz.), $\epsilon_r' \approx 10.2$, $\epsilon_r'' \approx 0.0235$, $h = 0.635$ mm, $\alpha = 5°$, $N = 36$ links. All dimensions on the layout are in mm.

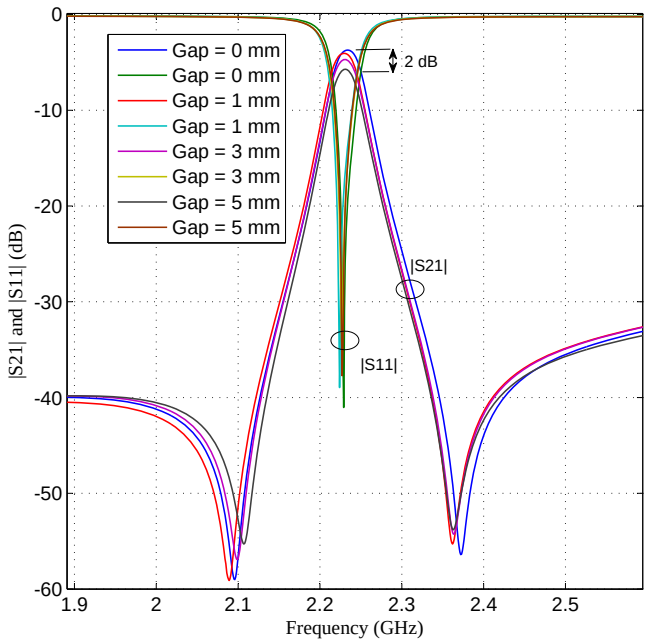

Fig. 12: FEM results for the 4 dual-mode filters designed in Fig. 11. Observed is the degradation in IL at the filter level, due to the reduction in Q_0 at the resonator level.

validates the generality of the used model. Two examples are considered: a square patch resonator and a line resonator (with its width much smaller than the wavelength). The geometric modifications applied follow the same principles developed in the previous sections. For the line resonator, the gaps are bridged when the links are present, maintaining the original resonator frequency, f_0. When the links are orderly removed (starting from the left side in Fig. 10c or Fig. 13b), the length of the line will be shortened, which will change its resonant frequency, f_0, to higher values.

Figs. 10b-c, 13 and 14 show the realization, layouts and the performances of the square and line resonators, respectively. Selected gap sizes (0, 1, 2, 4 mm) are shown for each case, with both theory predictions and measurement results compared. It is seen that good agreement exist between the results, within the fabrication tolerances. The only difference in the model application to these two cases, compared to the circular example, is that the normalised modal area, γ, under the dominant mode in equation (10) is now being calculated over the sum of aperture areas (S_i) which are rectangular in shape. The dominant modes that traverse these resonators (TM_{100} or TM_{010} for the square and TM_{100} for the line) are well-known and take the shape of half-sinusoids.

VII. Conclusion

Planar microwave and electromagnetic resonators which are customarily tuned geometrically often face performance degradation, expressed in reduced Q_0 values. Although this degradation is partly due to the imperfections in the tuning elements and materials normally used to achieve the tuning, it is also partly due to a significant reduction in the theoretical capability of the structure to store electromagnetic energy after the introduction of the tuning mechanism itself. This latter factor is always present, regardless of the quality of the tuning elements used, and is related to the resonant mode in question. This paper presents the electromagnetic theory behind this factor in general (even at frequencies above microwave frequencies), provides the physical explanation behind it, and demonstrates it in the microwave region through practical examples.

By applying this theoretical model onto planar resonator tuning problems, the designer is given a tool to assist in optimizing the tuning method geometrically. Depending on the desired behavior of Q_0 over the range of possible geometric modifications (which will always produce rolling-down Q_0 values but at controllable rates), the designer can choose the appropriate geometric tuning method that satisfies the design requirements. This provides insight and better understanding of the problem of geometric resonator tuning. Furthermore, the presented theory provides a useful electromagnetic model for

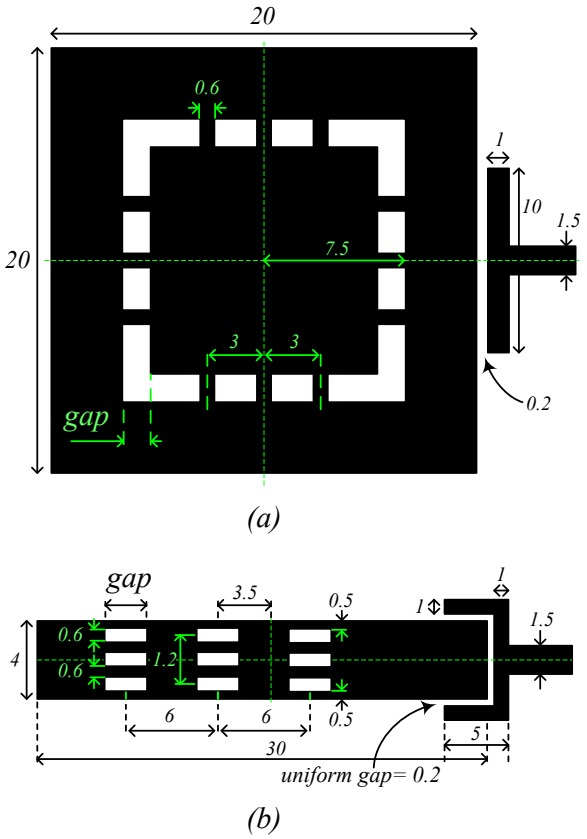

Fig. 13: Layouts of the (a) square patch resonator and (b) the line resonator, both with ideal links. Both setups had a variable *gap* size and used an Aluminum enclosure with dimensions 50 mm × 50 mm × 31 mm, copper metallic resonator and ground plane (0.5 oz.), $\epsilon_r' \approx 6.15$, $\epsilon_r'' \approx 0.0068$, $h = 0.635$ mm. All dimensions on the layouts are in mm.

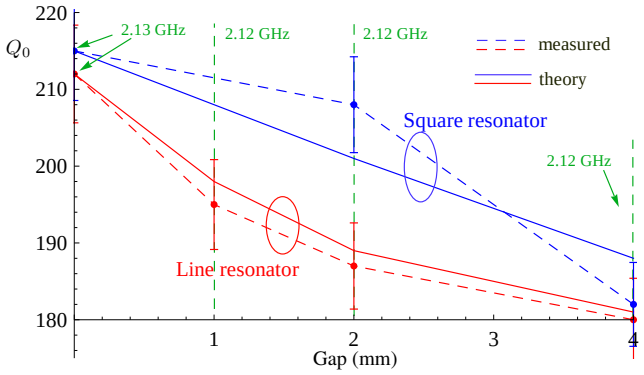

Fig. 14: Comparison between theory predictions and measurements for the square and line resonators shown in Figs. 10b-c and 13. Fabrication tolerances resulted in maximum errors circa ±3%.

estimating Q_0 for geometrically-modified or irregular metal patches and planar resonators in general, to assist analysis and design at any wavelength or application.

ACKNOWLEDGMENT

The authors would like to thank Nour AlShami and Rob Davies for their help fabricating the protoytpes.

REFERENCES

[1] S. Ramo, H. R. Whinnery, and T. Van Duzer, Eds., *Fields and Waves in Communication Electronics*, 3rd ed. Wiley, 1994.
[2] R. E. Collin, *Field Theory of Guided Waves*, 2nd ed. IEEE Publications, 1996.
[3] C. A. Balanis, *Antenna Theory: Analysis and Design*, 2nd ed. Wiley Blackwell, 1996-2005.
[4] R. E. Collin, *Foundations for Microwave Engineering*, 2nd ed. Wiley Blackwell, 2000.
[5] C. A. Balanis, *Advanced Engineering Electromagnetics*. John Wiley & Sons, 1989.
[6] J. G. Hong and M. J. Lancaster, *Microstrip Filters for RF/microwave Applications*. Wiley Blackwell, 2001.
[7] G. L. Matthaei, L. Young, and E. M. T. Jones, *Microwave Filters, Impedance-Matching Networks and Coupling Structures*. Artech House, 1980.
[8] C. G. Montgomery, R. H. Dicke, and E. M. Purcell, Eds., *Principles of Microwave Circuits*. Dover Publications Inc., 1965.
[9] H. Chen, L. Chan, and P. Sheng, "Transformation optics and metamaterials," *Nature Materials*, vol. 9, no. 5, pp. 387–396, May 2010.
[10] M. R. Dennis, "A cat's eye for all directions," *Nature Materials*, vol. 8, no. 8, pp. 613–614, 2009.
[11] Nikolay I. Zheludev, "What diffraction limits?" *Nature Materials*, vol. 7, pp. 420–422, June 2008.
[12] G. Lerosey, "Nano-optics: Yagiuda antenna shines bright," *Nature Photonics*, vol. 4, May 2010.
[13] D. M. Pozar, *Microwave Engineering*, 3rd ed. John Wiley & Sons, 2004.
[14] Y. Ma, C. Ong, T. Tyc, and U. Leonhardt, "An omnidirectional retroreflector based on the transmutation of dielectric singularities," *Nature Materials*, vol. 8, no. 8, pp. 639–642, 2009.
[15] I. Hunter, Ed., *Theory and Design of Microwave Filters*. 'The IET, 2001.
[16] G. M. Rebeiz, *RF MEMS: Theory, Design and Technology*. Wiley Blackwell, 2003.
[17] L. Dussopt and G. M. Rebeiz, "Intermodulation distortion and power handling in rf mems switches, varactors, and tunable filters," *IEEE Transactions on Microwave Theory and Techniques*, vol. 51, no. 4, pp. 1247–1256, Apr. 2003.
[18] P. Wong, I. Hunter, G. Rebeiz, K. Entesari, I. Reines, S.-J. Park, M. Tanani, A. Grichener, A. Brown, J.-S. Hong and R. Mansour, "Adapt to the app: Tunable and reconfigurable filters," *IEEE Microwave Magazine*, vol. 10, no. 6, 2009, special issue (no. 6).
[19] E. L. Ginzton, *Microwave Measurements*. McGraw-Hill, 1957.
[20] R. J. Cameron, R. Mansour, and C. M. Kudsia, *Microwave Filters for Communication Systems: Fundamentals, Design and Applications*. Wiley Blackwell, 2007.
[21] T. Lee, *Planar Microwave Engineering: A Practical Guide to Theory, Measurement, and Circuits*. Cambridge University Press, 2004.
[22] R. P. Owens, "Curvature effect in microstrip ring resonators," *Electronic Letters*, vol. 12, no. 14, pp. 356–357, 1976.
[23] I. Wolff and N. Knoppik, "Microstrip ring resonator and dispersion measurement on microstrip lines," *Electronic Letters*, vol. 7, no. 26, pp. 779–781, 1971.
[24] J. Watkins, "Circular resonant structures in microstrip," *Electronic Letters*, vol. 5, no. 21, pp. 524–525, 1969.
[25] Ansoft, "Asoft's website," http://www.ansoft.com.
[26] K. Chang, *Microwave Ring Circuits and Antennas*. John Wiley & Sons, 1996.
[27] www.NXP.com.

Adham Naji received his Bachelor's degree in Electronic Engineering from the University of Damascus in 2004, his M.Sc. (with distinction) in Digital Communications from the University of Bath in December 2005 and his Ph.D in Microwave and Electromagnetic Engineering from the University of Bristol in January 2010. His research interests include reconfigurable microwave resonator and filter design, electromagnetic wave theory, antenna design, complex analysis in optics and microwave theory, and microscopy (topics such as super-resolution).

Paul Warr received his B.Eng. (Electronics and Communications) from The University of Bath in 1994, and his M.Sc. (Communication Systems) and Ph.D. (Radio Frequency Engineering) from The University of Bristol in 1996 and 2001 respectively. He is currently a Senior Lecturer in Electronics at the University of Bristol where his research covers the front-end aspects of Software-Defined Radio.

Mark Beach Mark Beach received his PhD for research addressing the application of Smart Antennas to GPS from the University of Bristol in 1989, where he subsequently joined as a member of academic staff. He was promoted to Senior Lecturer in 1996, Reader in 1998 and Professor in 2003. His research interests include the application of multiple antenna technology to enhance the performance of wireless systems.

Kevin Morris received his B.Eng. and Ph.D. degrees in electronics and communications engineering from the University of Bristol in 1995 and 1999, respectively. He became a research associate at the University of Bristol in 1998, and worked on a number of projects including the EPSRC PACT LINK program and the IST project SUNBEAM. He is currently a senior lecturer in radio frequency engineering and is involved with a number of EPSRC and industrial research programmes. His research interests are in the area of radio frequency hardware design.